STUDY THE OPTICAL PROPERTIES OF COPPER OXIDE THIN FILM DEPOSITED BY COLD SPRAY

Samir H. Awad **Riyam I. Jadaan**

ABSTRACT:

Copper oxide (CuO) thin films were prepared by cold spray process using inert atmosphere (helium gas) without employing any catalyst. CuO dry powder was sprayed onto microscope glass slide by heating carrier gas at 100, 200, 300, and 400 °C ,with 30 bar gas pressure onto substrates of 300 ± 5°C at different angles 0°, 30°, 45°, then study the effect of these parameter on the structural, and optical properties of the resulted thin film. The X-ray diffraction (XRD) studies showed that the as-deposited CuO has the monoclinic structure with low strain. SEM images show that the thin film has no porosity or agglomeration and deposit on the entire region. The CuO thin film exhibited a high transmittance of about (96%).

Key words: TCO materials; Optical properties; CuO; Cold spray process.

دراسة الخواص البصرية لأغشية أوكسيد النحاس الرقيقة المرسبة بالرش البارد

سمير حامد عواد **ريام عماد جدعان**

الخلاصة

تم ترسيب أغشية أوكسيد النحاس باستخدام طريقه الرش البارد عن طريق استخدام غاز خامل (غاز الهليوم) بدون استخدام أي مواد مساعدة. حيث تم رش مسحوق أوكسيد النحاس الجاف على أرضيات زجاجية المسخنة بدرجه حرارة 300درجه مئوية بواسطة تسخين الغاز بدرجات (100,200,300,400) درجة مئوية بضغط 30 بار بزوايا ترسيب مختلفة (0, 30, 45) .بعدها تم دراسة تأثير هذه المتغيرات على الخواص التركيبية والبصرية للأغشية الناتجة .حيث اظهرت نتائج حيود الاشعه السينيه أن الاغشيه المترسبه تمتلك تركيب أحادي الميل .أما صوره المجهرالالكتروني الماسح فاظهرت بان الغشاء لا يحوي على اي مسامات او تكتلات وان المسحوق مترسب على كل الارضيه .و الغشاء يمتلك شفافيه عاليه تصل الى (96%).

1- INTRODUCTION

In recent years, the synthesis of nanostructured thin films of a semiconductor and metal oxides has attracted an increasing attention due to their excellent electronic and optical properties compared with those of the corresponding bulk materials [1]. The current challenges are to find methods to synthesis of these materials with controlled characteristics of size, phase, morphology, composition and good levels of purity to generate thin films [2,3], one of these methods is the cold spray where the worldwide interest in the cold spray technique has led to significant research effort, both in the design of equipment and methods to make it more simple and efficient [4]. This method is totally different from other coating processes because the use of low temperatures where low temperature aids in retaining the original powder chemistry and phases in the coating, with changes only due to deformation and cold-working [5]. And prevent stress generation which always induces after the significant change in the temperature [4]. Also this process has another feature which is it low cost in comparison with other thermal spray method [6]. Oxides of copper are known to show p-type conductivity and are attracting renewed interest as promising TCO materials in the fabrication of a wide range of optoelectronic devices. Nontoxic, economic and abundant availability and relatively simple formation of oxide makes copper oxide as an interesting material [7]. Cuprous oxide (Cu_2O) and cupric oxide (CuO) are the two main semiconductor phases of copper oxide with narrow band gap [8]. Compared with Cu_2O, CuO is more stable and more easily prepared. Its band gap matches the spectrum of sunlight more closely, allowing it to absorb more sunlight. These characteristics make it more suitable for solar cell applications [9]. CuO is unique as it has a square planar coordination of copper by oxygen in the monoclinic structure. The lattice parameters of CuO are a= 4.6837A˚, b= 3.4226A˚, c= 5.1288A˚[10,11].

2. EXPERMENTAL DETALES

2-1 Thin Film Deposition

CuO films have been produced by spraying copper oxide powder onto the microscope glass substrates (1x25x75mm^3) at substrate temperature of 300°C. Prior to deposition, the substrates were cleaned with acetone and ethanol alcohol, washed with de-ionized water (non-ionized) followed by a wet soft tissue [12]. The powder that used is cupric oxide (CuO) with particle size 200 mesh (78μm), origin (wenger materials for craft pottery), with purity 96%. The copper oxide powder was ground for 8 hour using Ball Mill type (9VS, CAPCO test equipment Ltd. UK), to obtain the desire particle size. After ground of the powder the study of particle size and particle size distribution was made through a Laser Diffraction Particle Size Analyzer (type 2000 Bettersize Instrument Ltd. ,China). The home-made cold spray apparatus was fabricated and built, as shown in **(Figure 1)**.

The prepared substrates are fixed onto electric heater, the growth of copper oxide microstructures were carried out by spray of powders in an inert atmosphere (Helium gas) at conditions shown in **(Table 1)**. Subsequently develops a nanocrystalline layer at substrate with temperature of 300℃ [13,14]. After the deposition process, the samples were annealed in vacuum furnace (GSL-1500X MTI CORPORATION, USA) The samples were annealed at 450°C [12, 15] for 30 min at a rate of 20 °C.min^{-1} under vacuum of 0.5×10^{-3} Torr.

2- 2 Structural Characterization

Crystal structure were investigated by means of a X-ray diffraction XRD Shimadzu 6000 Japan using CuKα1, (λ=1.5405Å, 30mA, 40 kV) in 2Θ range from 20˚ to 70˚.

2-3 Optical Transmission Measurement

The optical transmittance of the copper oxide films was studied in the wavelength range from (300 - 1100nm) at room temperature. By using UV-VIS-NIR spectrophotometer (type SP8001 Metertech, USA).

2-3-1 The Absorption Coefficient (α) Measurement

The absorption coefficient can be define as a measure of the rate of decrease in the intensity of electromagnetic radiation (as light) as it passes through a given substance ,or it is the fraction of incident radiant energy absorbed per unit mass or thickness of an absorber [16]. It is important to calculate The absorption coefficient in order to know the nature of the electron transition, if the value of measured α is high, as ($\alpha > 10^4\ cm^{-1}$) then the transition is direct, while if the value of measured α is low, as ($\alpha < 10^4\ cm^{-1}$) then the transition is indirect [17], also the value of absorption coefficient refer to the ability of thin film material to absorbs the incident radiation [16].

The absorption coefficient can be determined by Beer–Lambert law [18]:

$$I = I_o e^{-\alpha t} \quad (1)$$

Where: I is the intensity of transmitted UV spectrum, I_o is the intensity of UV entering the material (excluding surface reflection), α is the absorption coefficient in inverse length units, t is the thickness of the thin film [18].

Since A is ($log \frac{I_o}{I}$) and it represent the absorption of thin film, α can be rewritten as [18]:

$$\alpha = \frac{2.03\ A}{t} \quad (2)$$

2-3-2 Optical Band Gap (E_g) Measurement

The optical absorption is dominated by the optical band gap (E_g) of the semiconductor that is related to the optical absorption coefficient (α) and the incident photon energy (hv) by using Tauc equation [18]:

$$(\alpha hv) = A(hv - E_g)^n \quad (3)$$

where α is absorption coefficient, A is constant (independent from ν) and *n* the exponent that depends on the kind of optical transition (n = 1/2, 2 when the transition is direct-allowed, indirect-allowed respectively).

The photon energy (hν) can be calculated using [19]:

$$E = hv = \frac{hc}{\lambda} \quad (4)$$

where h is Plank's constant ($6.626x10^{-34}$), c is speed of light ($3x10^{8}$) and λ is the wavelength [20].

2-4 Surface Morphology

To study the surface topography and morphology of films, Scanning Electron Microscope (SEM) type (Tescan VEGA Easy Probe ,CZ - Europe), were used. The thickness of the film was monitored using depth profiler probe (PF probe) type (Angstrom Sun Technologies Inc., USA).

3- RESULTS AND DISCUSSION

3-1 Laser Diffraction Particle Size Analyzer for CuO Powder

(Figure 2) show Particle size distribution of the CuO powder, it is possible to observe that the differential volume has a Gaussian distribution and the accumulated volume is expressed in a continuous line. The statistic of the particle size distribution can be found in **(Table 2)** ,where it can be seen that 80% of the particles are between 1.797 μm and 19.55 μm with a mean size of 10 μm .

This powder presents a size in the range of the ideal size (1-50μ) of cold spray process. Also, it has a narrow size distribution (0.8-28μm), therefore the particles may present the same impact velocity, by having the same weights, so it will impact the substrate at the same velocities because they can reach the same kinetic energy.

3-2 Structural Properties

(Figure 3) shows XRD patterns for CuO thin films, deposited onto substrate in the 2θ range (20˚ -70˚). Pattern indicated that there are two sharp reflection peaks ($\bar{1}11$) and (111) at 35.552° and 38.75° respectively and the film was polycrystalline in nature. The monoclinic structure was matched with the standards peaks (ASTM - Card file No. 00-005-0661).

3-3 Optical Properties

3-3-1 Transmittance

(Figure 4) shows the relationship between the optical transmittance and wavelength of the CuO thin films deposited on the glass substrate at different deposition temperatures. The value of the optical transmission increased with increasing temperature of the deposition in the ultraviolet and visible regions because as the temperature increase the grain size increase and the grain boundary decrease (which act as a scattering center) so that the light will pass without disperse, and when the wavelength is increase at near infrared region we notice that the thin film which deposits at 400℃ has a little increase compared with other deposited thin film because increasing the deposition temperature leads to the regularity of the structure. **(Figure 5)** shows the relationship between transmittance with wavelength of CuO thin films, deposited on the glass substrate at different deposition angles. The value of transmittance increases with increasing angle of deposition, because the light does not disperse when passed through the film. The optimum optical transmittance was found for the thin film formed on a glass substrate at (200 °C and 45°). As shown in **(Figures 4 and 5)**, an average transmission of about 96% was observed for the CuO thin in the visible regain.

3-3-2 The Absorption Coefficient (α)

(Figure 6) shows the variation of absorption coefficient with the photon energy for CuO at different temperature . It can be noticed that the absorption coefficient increased with photon energy increasing . **(Figure 7)** shows the variation of absorption coefficient with the photon energy for CuO at different angle and temperature fixed at 200℃, it is clear to see that the absorption coefficient decrease as the angle increase .From the previous **(Figures 6 and 7)** it can be concluded that the thin film has two type of electron transition (direct , indirect).

3-3-3 Energy band gab (Eg)

3-3-3-1 Effect of Temperature Variation on the Energy Band Gab (Eg)

The direct allowed energy band gab (Eg) can happened if the transition between the upper limited of covalent band and the lower limited of conductive band. The **(Figures 8, 9, 10, and 11)** indicate that the energy gab affects with the deposition temperature where the energy band gab (Eg) value is found to be (2.35 eV –1.99 eV). Where at 100℃ we notice that the Eg is (2.35 eV), 200℃ (2.349 eV) , 300℃ (2.3 eV) ,and 400℃ (1.99 eV). this decrease in Eg value because the decrease in localize state inside the energy band gab which may found because defect in the structure.

The indirect allowed energy band gab (Eg) can happened if the transition in places near the direct allowed. The coming **(Figures 12 ,13 ,14 ,and 15)** indicate that the energy gab affects with the deposition temperature where the energy band gab (Eg) value is found to be (1.25 eV – 1.12 eV) Where at 100℃ we notice that the Eg is (1.25 eV), 200℃ (1.18 eV) , 300℃ (1.2 eV) ,and 400℃ (1.12 eV), this decrease in Eg value because decrease in localize state inside the energy band gab which may found because defect in the structure.

3-3-3-2 Effect of Angle Variation on the Energy Band Gab (Eg)

The **(Figures 16 ,17 ,and 18)**, indicate that the energy gab effects with the deposition temperature where the energy band gab (Eg) value is found to be (2.349 eV –2.46 eV). Where at 0˚ we notice that the energy band gab (Eg) is (2.349 eV), 30˚ (2.4 eV) ,and 45˚ (2.46 eV),there is an increase in the energy band gab value.

The coming **(Figures 19, 20, and 21)**, indicate that the energy gab affects with the deposition temperature where the energy band gab (Eg) value is found to be (1.18 eV -1.55 eV). Where at 0˚ we notice that the energy band gab (Eg) is (1.18 eV), 30˚ (1.51 eV) ,and 45˚ (1.55 eV), there is an increase in the energy band gab value.

The calculated band gab are collected in **(Table 3)**, to show the variation of band gab with deposition temperature and the deposition angle in easy way.

3-4 surface properties

(Figures 22) shows image of SEM for prepared CuO thin films. It is clear that the CuO thin films have distributed over the entire area with no porosity or agglomeration.

The thin film thickness is 100 nm.

4- Conclusions

1-Copper oxide thin films crystals with a monoclinic structure, were deposited by cold spray process and no template or catalyst was used.

2-The XRD results of the thin films crystals found that the thin films are consistent with the structure of monoclinic.

3-The optical transmittance for CuO thin film increased with increasing temperature of the deposition in the ultraviolet region and visible light with an average visible transmittance 96%, also it increased with increasing angle of the deposition because the deposition efficiency increase.

4- The absorption coefficient increase with photon energy, also it is notice that the thin film behave two type of electron transition (direct , indirect). The value of calculate energy gab is in the range of CuO.

5- The obtain Copper oxide produce in this work consider to be a (TCO) Transmittance Conductive Oxide, and all those result make copper oxide suitable material as windows for solar cell.

5- References

[1] I. Bobowska , P. Wojciechowski "Synthesis of nanostructures of copper compounds and their hybridisation with titanate nanosheets" Journal of Crystal Growth ,no.312 685–691(2010).

[2] M. Mukundan," Phase Control in the Synthesis of Yttrium Oxide Nano and Micro-particles by Flame Spray Pyrolysis", M.Sc. Thesis, Texas A&M University, August 2007.

[3] R. Kavitha, S.R. Hegde, Vikram Jayaram," Oxide films by combustion pyrolysis of solution precursors", Materials Science and Engineering, A359, 18-23(2003).

[4] Maria Manuel Fernandes Barbosa, "Cold Spray Deposition of Titanium onto Aluminium Substrates" Msc. Thesis ,university of Porto , Portugal.

[5] R. Ghelichi , S. Bagherifard , M. Guagliano , M. Verani "Numerical simulation of cold spray coating" Surface & Coatings Technology, No. 205 ,5294–5301(2011).

[6] M. Grujicic , V. Sellappan, L. Mears, X. Xuan, Norbert Seyr, Marc Erdmann, Jochen Holzleitner " Selection of the spraying technologies for over-coating of metal-stampings with thermo-plastics for use in direct-adhesion polymer metal hybrid load-bearing components" journal of material processing technique, No198, 300–312 (2008).

[7] V. Figueiredo, E. Elangovan , G. Gonçalves , P. Barquinha , L. Pereira, N. Franco, E. Alves , R. Martins , E. Fortunato " Effect of post-annealing on the properties of copper oxide thin films obtained from the oxidation of evaporated metallic copper" Applied Surface Science No. 254, 3949–3954(2008).

[8] Muslem F. Jawad , Raid A. Ismail , Khaled Z. Yahea "Preparation of nanocrystalline Cu_2O thin film by pulsed laser Deposition" J Mater Sciences: Mater Electron No 22 ,1244–1247 (2011).

[9] Fei Gao, Xiao-Jing Liu, Jun-Shan Zhang, Mei-Zhou Song, and Ning Li "Photovoltaic properties of the p-CuO/n-Si heterojunction prepared through reactive magnetron sputtering" J. Appl. Phys. 111, 084507 (2012).

[10] P A Korzhavyi, B Johansson" Literature review on the properties of cuprous oxide Cu_2O and the process of copper oxidation" Technical Report TR-11-08(2011).

[11] B. K. Meyer, A. Polity, D. Reppin, M. Becker, P. Hering, P. J. Klar, Th. Sander, C. Reindl, J. Benz, M. Eickhoff, C. Heiliger, M. Heinemann, J. Bläsing, A. Krost, S. Shokovets, C. Müller, and C. Ronning "Binary copper oxide semiconductors: From materials towards devices" Phys. Status Solidi B 249, No. 8, 1487–1509 (2012).

[12] Mohd Rafie Johan, Mohd Shahadan Mohd Suan, Nor Liza Hawari, Hee Ay Ching "Annealing Effects on the Properties of Copper Oxide Thin Films Prepared by Chemical Deposition" International Journal of Electrochemical Science, No. 6, 6094 – 6104 (2011).

[13] Iqbal Singh, R.K. Bedi "Studies and correlation among the structural, electrical and gas response properties of aerosol spray deposited self assembled nanocrystalline CuO" Applied Surface Science No. 257, 7592–7599(2011).

[14] Issam M. Ibrahim, Muhammad O. Salman, Ahmed S. Ahmed "Electrical behavior and Optical Properties of Copper oxide thin Films" Baghdad Science Journal Vol.8(2)2011.

[15] V. Figueiredo, E. Elangovan , G. Gonçalves , P. Barquinha , L. Pereira, N. Franco, E. Alves , R. Martins , E. Fortunato " Effect of post-annealing on the properties of copper oxide thin films obtained from the oxidation of evaporated metallic copper" Applied Surface Science No. 254, 3949–3954(2008).

[16] أ.م صبرية عليوي ضبع , د.فاتن شكور زين العابدين , د.انتصار هاتو هاشم " دراسة تأثير التلدين على الثوابت البصرية لأغشية CuO المشوبة بالانديوم" journal of college of education, No.1 ,2008.

[17] G. Busch and H. Schade, "Lectures on solid state physics", Pergaman Press, London, (1976).

[18] لمياء خضير عباس " دراسة تأثير السمك على الخواص البصرية لأغشية CuO المحضرة بطريقة الرش الكيميائي الحراري " مجلة أم سلمة للعلوم المجلد 3 (1) 2006.

[19] Mohd Rafie Johan, Mohd Shahadan Mohd Suan, Nor Liza Hawari, Hee Ay Ching "Annealing Effects on the Properties of Copper Oxide Thin Films Prepared by Chemical Deposition " International Journal of Electrochemical Science, 6 (2011) 6094 – 6104.

Table (1): Typical range of parameters for cold spray process.

parameters	*Range*
Operation gases	Helium gas (He).
Substrate temperature(℃)	300 [13,14]
Gas pressure (bar),without catalyst	30
Gas temperature (℃)	100, 200, 300, 400
Spray distance (mm)	40 [4]
Power consumption(for heat gas) (Kw)	3
Powder feed rate (g/s)	0.3
Deposition angles (°)	0, 30, 45

.**Table (2):** Statistics of the particle size distribution of the CuO powder.

Parameters	Result
Mean particle size	10 µm
Diameter correspondent to 10% accumulated volume	1.797 µm
Diameter correspondent to 50% accumulated volume	8.263 µm
Diameter correspondent to 90% accumulated volume	19.55 µm

Table (3): Optical band gap (Eg) values for copper oxide thin films.

Parameter	Direct-allowed energy gab (eV)	Indirect-allowed energy gab (eV)
100℃	2.35	1.25
200℃	2.349	1.18
300℃	2.3	1.2
400℃	1.99	1.12
0˚	2.349	1.18
30˚	2.4	1.51
45˚	2.4	1.55

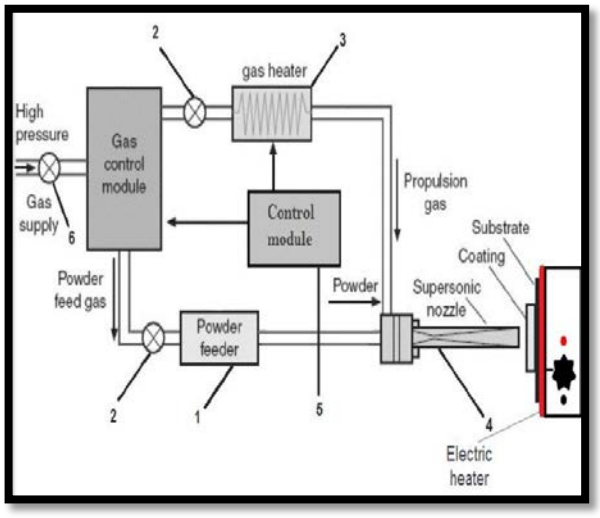

Figure (1): Schematic diagram of a cold spray system.

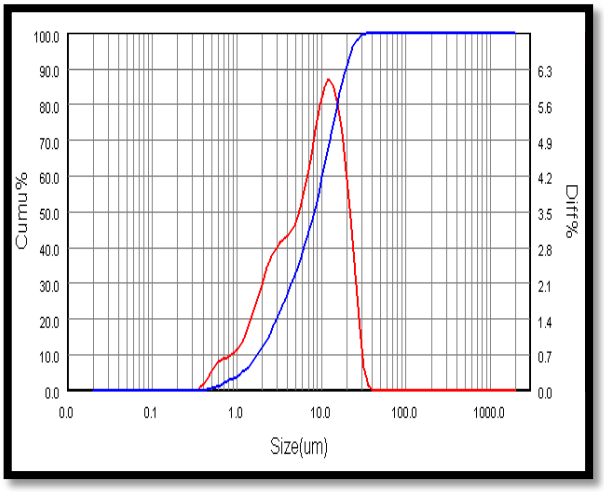

Figure (2): Particle size distribution of the CuO powder

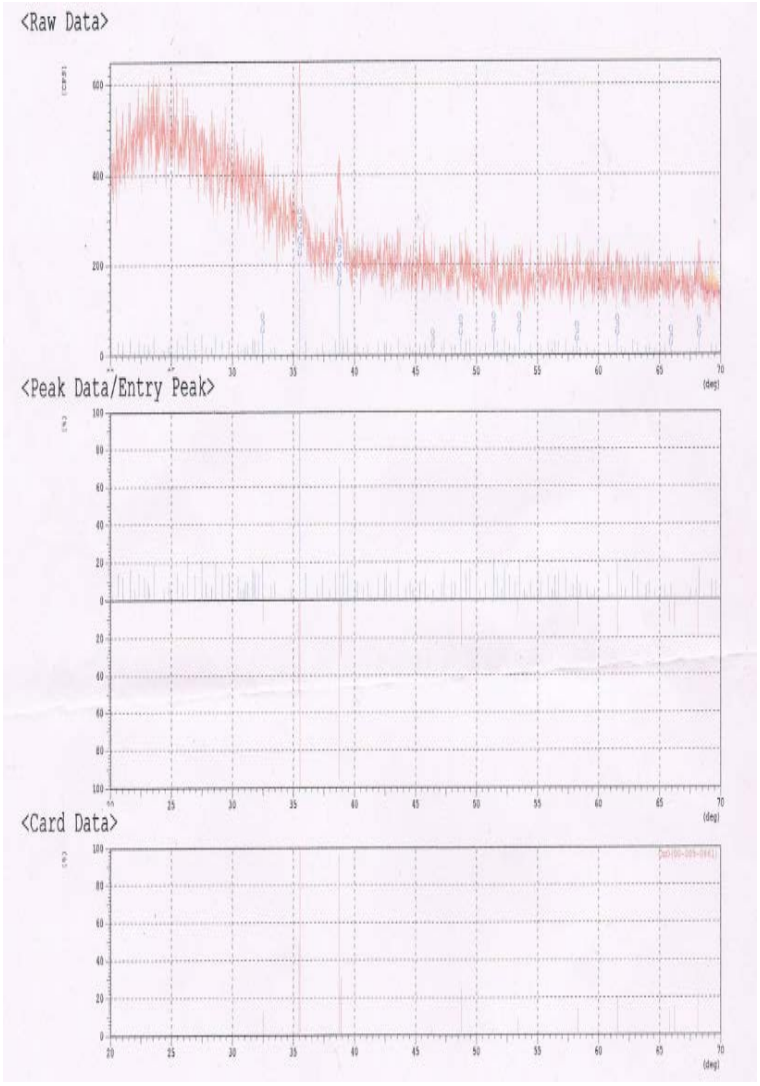

Figure (3): The XRD patterns of the CuO thin films.

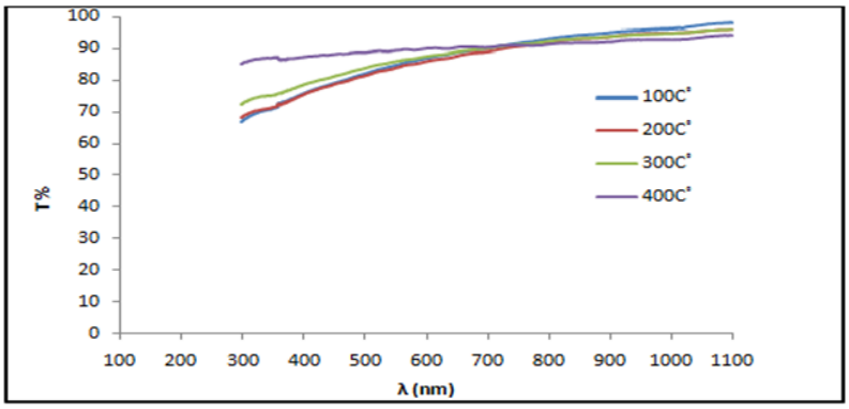

Fig (4) the relationship between the optical transmittance and wavelength for CuO thin films at different temperature.

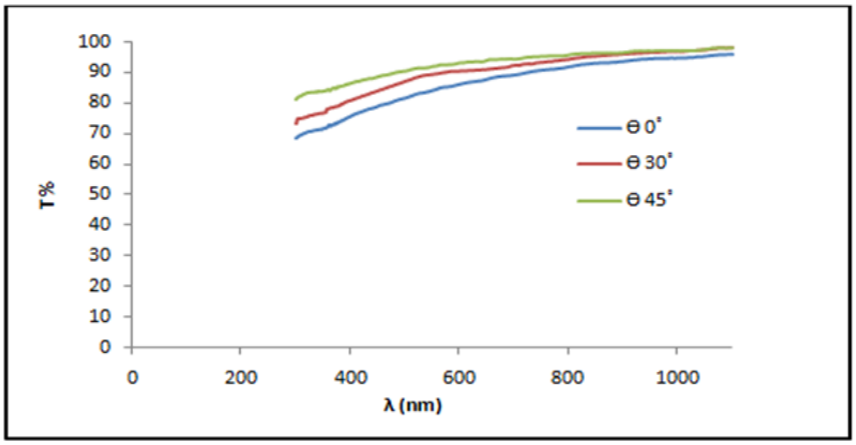

Figure(5) the relationship between of the optical transmittance and wavelength for CuO thin films at different angle and fixed temperature at 200°C.

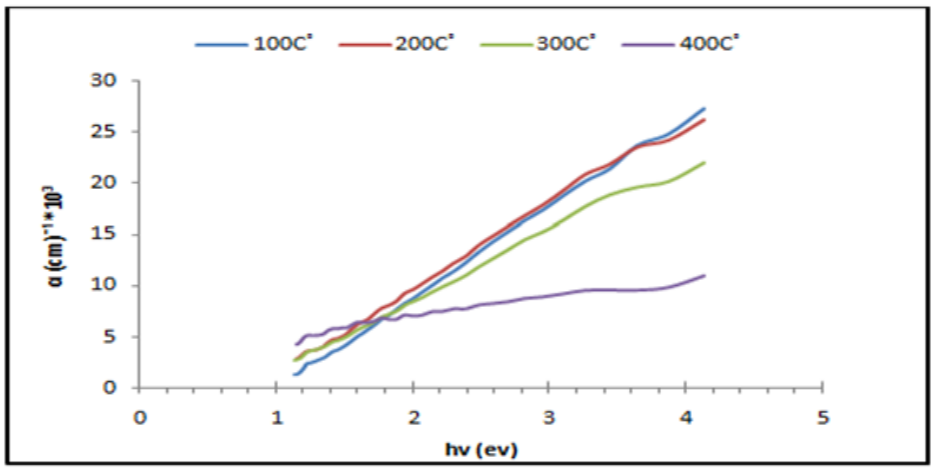

Figure(6) the variation of absorption coefficient with the photon energy for CuO at different temperature .

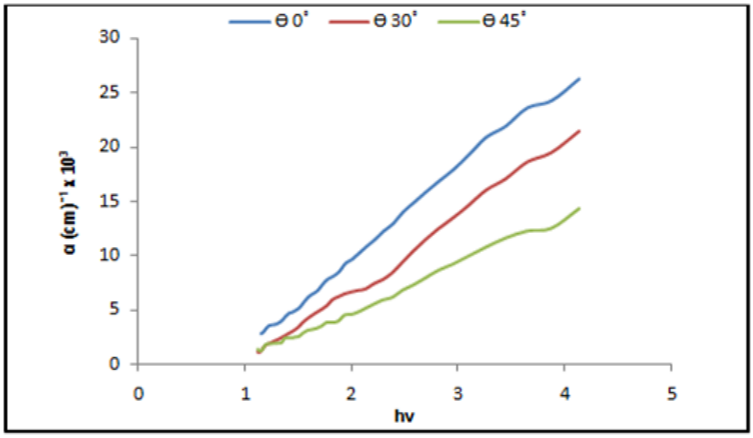

Figure (7) the variation of absorption coefficient with the photon energy for CuO at different angle and temperature fixed at 200°C .

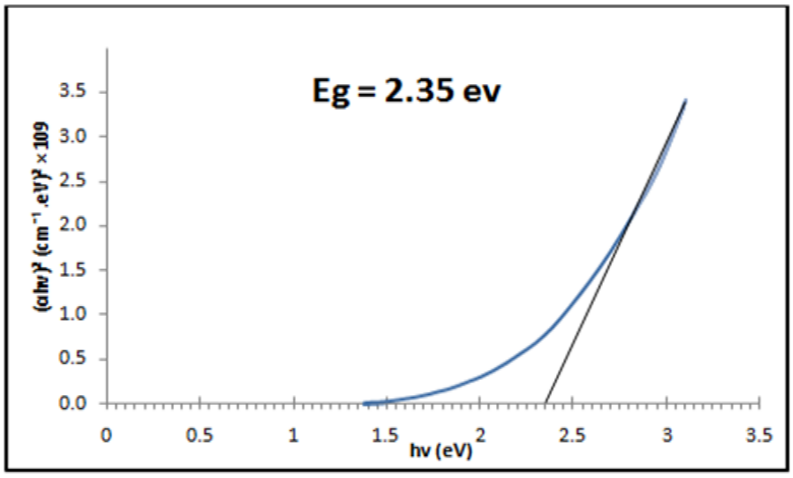

Figure (8) The variation of $(\alpha h\upsilon)^2$ versus photon energy ($h\upsilon$) for CuO films at 100°C .

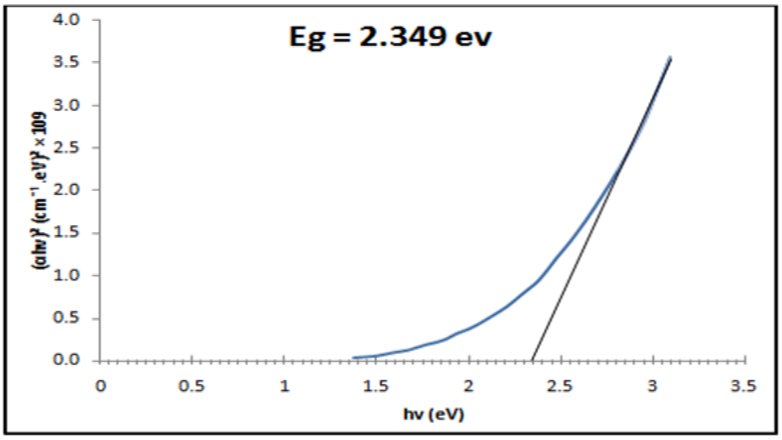

Figure (9) The variation of $(\alpha h\upsilon)^2$ versus photon energy ($h\upsilon$) for CuO films at 200°C

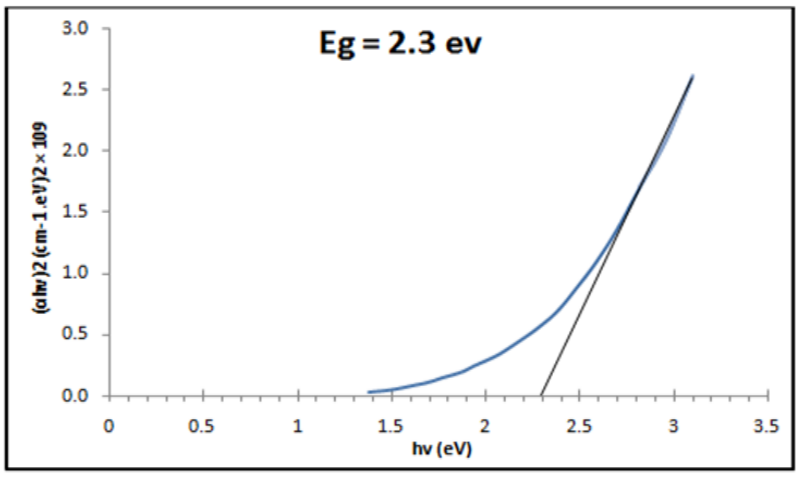

Figure (10) The variation of $(\alpha h\upsilon)^2$ versus photon energy ($h\upsilon$) for CuO films at 300°C .

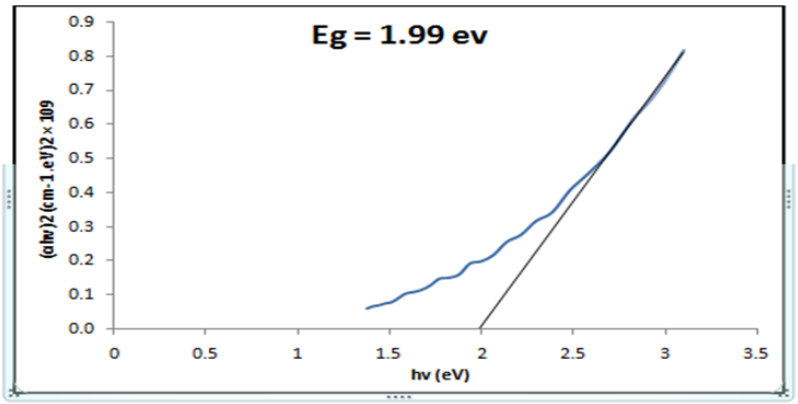

Figure (11) The variation of $(\alpha h\upsilon)^2$ versus photon energy ($h\upsilon$) for CuO films at 400°C .

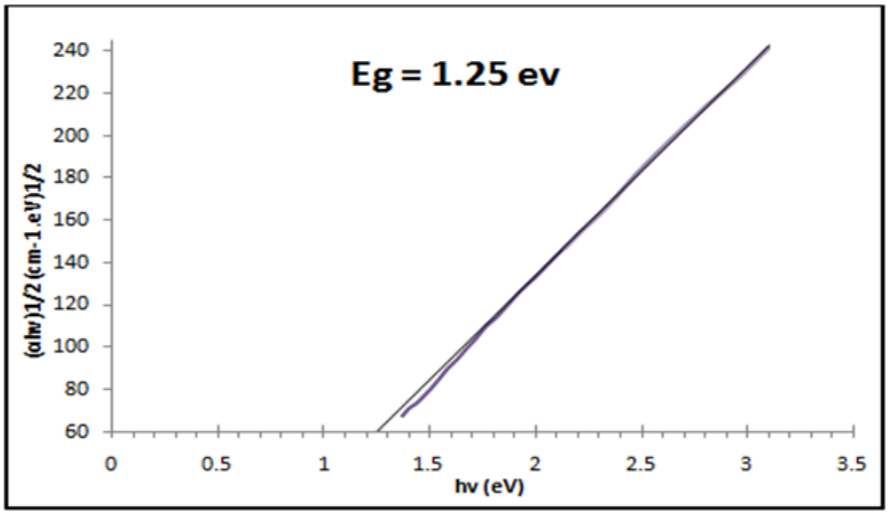

Figure(12) The variation of $(\alpha h\upsilon)^{\frac{1}{2}}$ versus photon energy ($h\upsilon$) for CuO films at 100°C

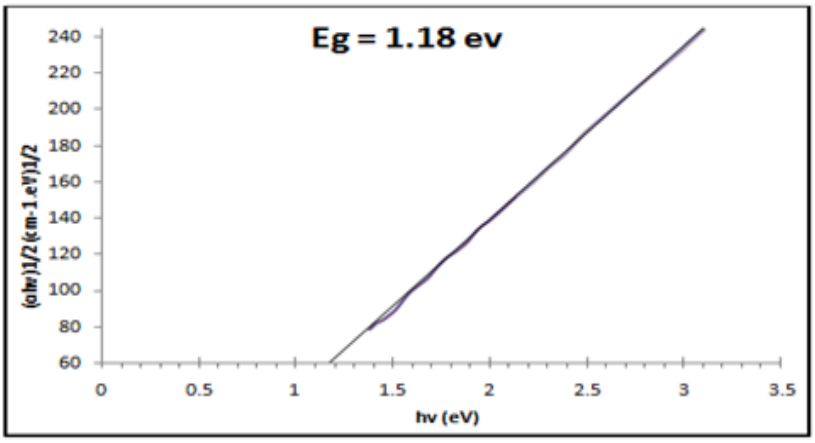

Figure(13) The variation of $(\alpha h\upsilon)^{\frac{1}{2}}$ versus photon energy ($h\upsilon$) for CuO films at 200°C

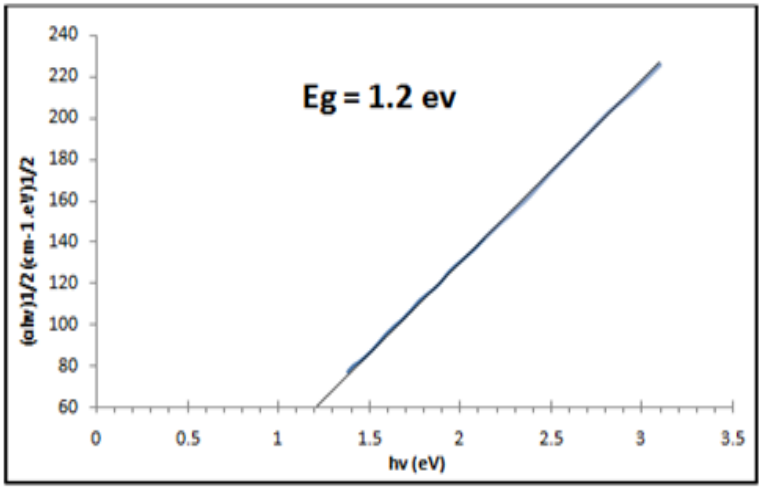

Figure (14) The variation of $(\alpha h\upsilon)^{\frac{1}{2}}$ versus photon energy ($h\upsilon$) for CuO films at 300°C .

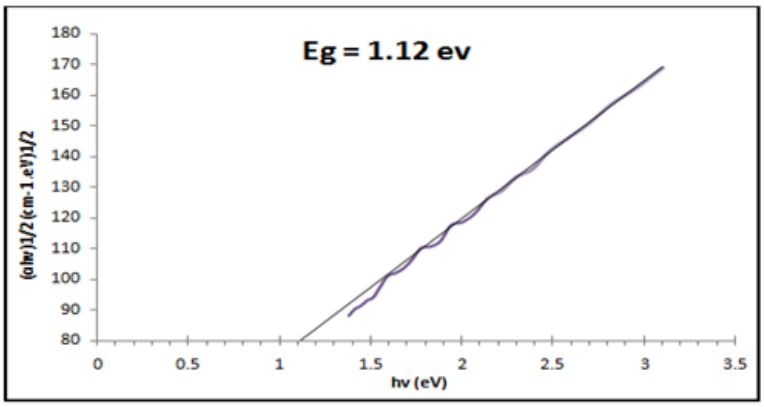

Figure (15) The variation of $(\alpha h\upsilon)^{\frac{1}{2}}$ versus photon energy ($h\upsilon$) for CuO films at 400°C

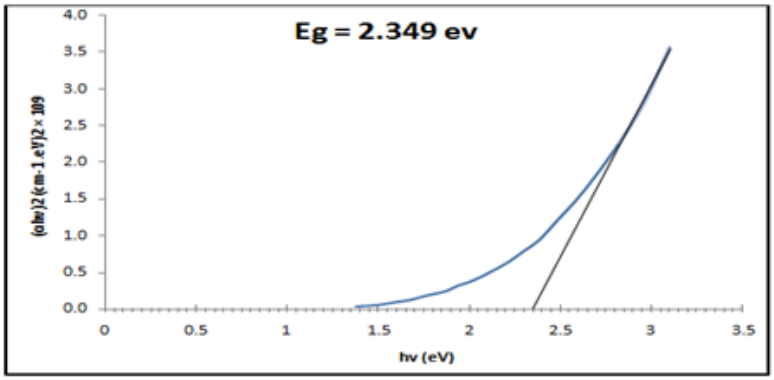

Figure (16) The variation of $(\alpha h\upsilon)^2$ versus photon energy ($h\upsilon$) for CuO films 0° .

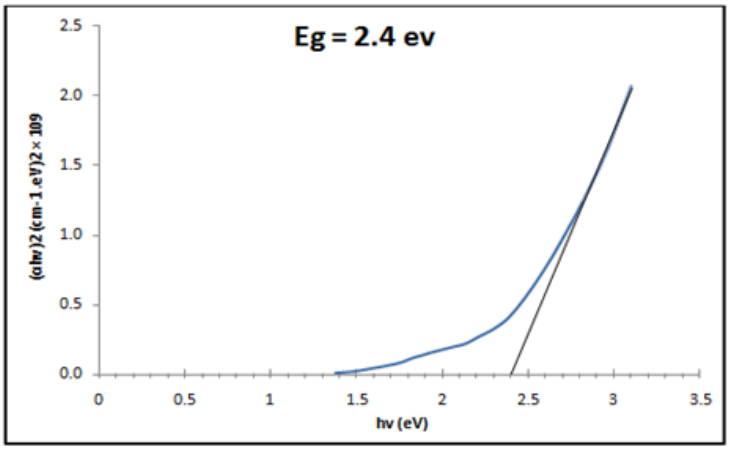

Figure (17) The variation of $(\alpha h\upsilon)^2$ versus photon energy ($h\upsilon$) for CuO films at 30°

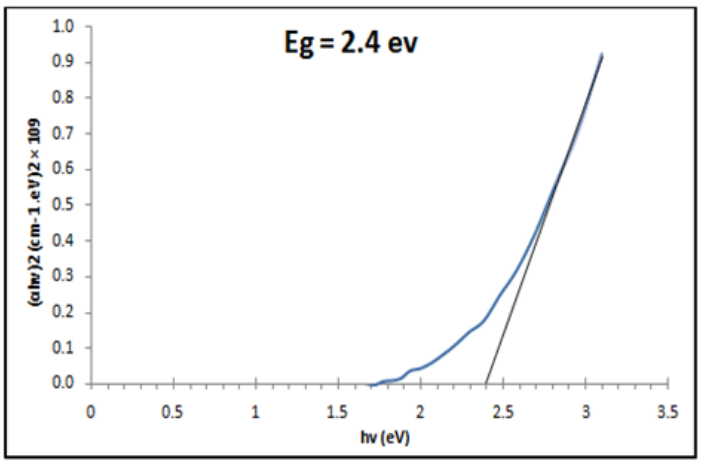

Figure (18) The variation of $(\alpha h\upsilon)^2$ versus photon energy ($h\upsilon$) for CuO films at 45° .

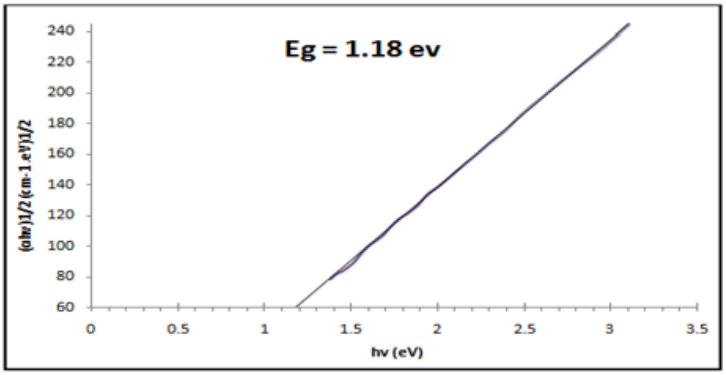

Figure (19) The variation of $(\alpha h\upsilon)^{\frac{1}{2}}$ versus photon energy ($h\upsilon$) for CuO films at 0° .

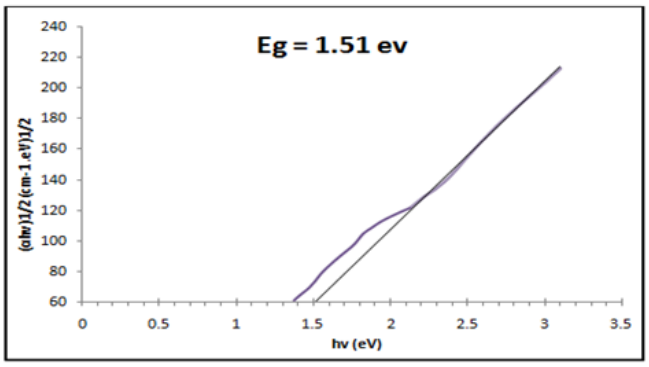

Figure(20) The variation of $(\alpha h\upsilon)^{\frac{1}{2}}$ versus photon energy ($h\upsilon$) for CuO films at 30° .

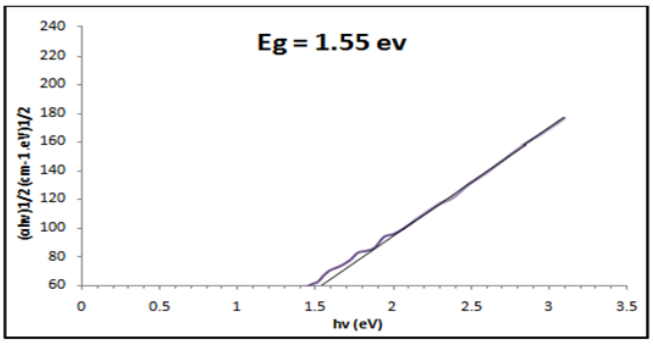

Figure (21) The variation of $(\alpha h\upsilon)^{\frac{1}{2}}$ versus photon energy ($h\upsilon$) for CuO films at 45° .

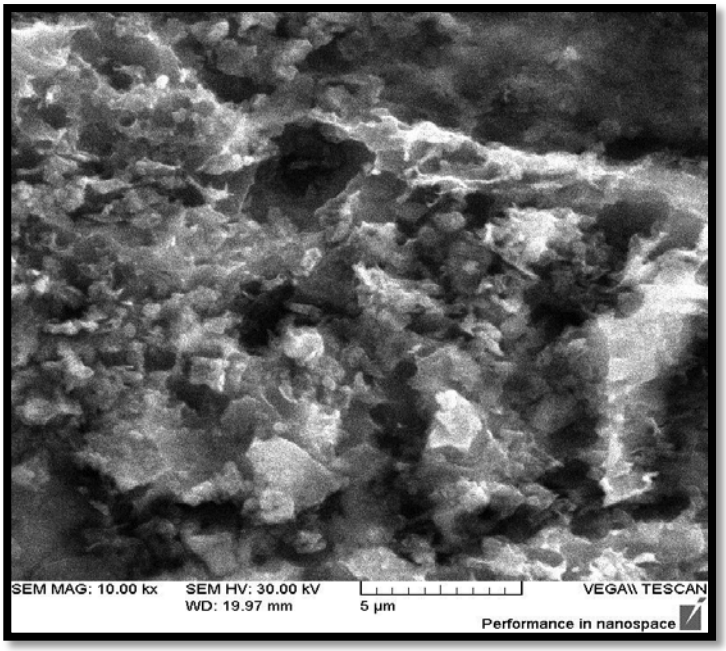

Figure (22): SEM image of CuO thin film onto glass substrate at deposition temperature 200°C.